DALTON
FULL PAPER

Synthesis and crystal structures of cationic lanthanide(III) monoporphyrinate complexes

Wai-Kwok Wong,*[a] Lilu Zhang,[a] Wing-Tak Wong,[b] Feng Xue[c] and Thomas C. W. Mak[c]

[a] *Department of Chemistry, Hong Kong Baptist University, Kowloon, Hong Kong*
[b] *Department of Chemistry, The University of Hong Kong, Pokfulam Road, Hong Kong*
[c] *Department of Chemistry, The Chinese University of Hong Kong, Shatin, N.T., Hong Kong*

Received 14th December 1998, Accepted 14th December 1998

Reactions of an excess of $Ln[N(SiMe_3)_2]_3 \cdot x[LiCl(THF)_3]$, generated *in situ* from the reaction of anhydrous $LnCl_3$ with 3 equivalents of $Li[N(SiMe_3)_2]$ in tetrahydrofuran, with 5,10,15,20-tetrakis(*p*-methoxyphenyl)porphyrin (H_2TMPP) in refluxing tetrahydrofuran–bis(2-methoxyethyl) ether solution (1 : 6 v/v) gave the cationic monoporphyrinate complexes $[Ln^{III}(TMPP)(H_2O)_3]Cl$ (Ln = Yb; **1**, Er, **2**, or Y **3**), and with 5,10,15,20-tetrakis(*p*-tolyl)-porphyrin (H_2TTP) gave $[Yb^{III}(TTP)(H_2O)_2(THF)]Cl$ **4**. The structures of compounds **1**–**4** have been established by X-ray crystallography. Metathesis of **1** with an excess of $AgBF_4$ gave the unexpected neutral monoporphyrinate complex $[Ag^{II}(TMPP)]$ **5** whose structure was also determined. Compound **1** catalysed the cyclotrimerization of phenyl isocyanate.

Lanthanide(III) monoporphyrinate complexes were first reported in 1974.[1a] However, since then only a few studies on these systems have appeared in the literature.[1] Although the structural data of lanthanide(III) bis(porphyrinates)[2] and porphyrin-phthalocyanine[3] heteroleptic sandwich complexes are well documented, structural characterization of the neutral lanthanide(III) monoporphyrinate complexes of lutetium[4] and terbium[5] was accomplished only recently. However, to our knowledge, there is no report on cationic lanthanide(III) monoporphyrin complexes in the literature. We are interested in the chemistry of this type of complex, particularly regarding their potential as Lewis acid catalysts for chemical transformations. Lanthanide alkyls and amides are very reactive species and good precursor complexes for the preparation of organolanthanide complexes. Recently, protonolysis of lanthanide alkyls with porphyrin free bases has been used to synthesize lanthanide monoporphyrinate complexes.[4] However, the utilization of lanthanide amide analogues for the preparation of lanthanide porphyrin complexes has not been reported. We would like to explore the possibility of using lanthanide amide complexes as precursors for the preparation of cationic lanthanide porphyrin complexes *via* the route (1).

$$Ln(NR_2)_3 + H_2porp \longrightarrow [Ln(porp)(NR_2)] \xrightarrow{H_2O/X^-} [Ln(porp)]X + R_2NH \quad (1)$$

We herein report the reactions of $Ln[N(SiMe_3)_2]_3 \cdot x[LiCl(THF)_3]$, generated *in situ* from the reaction of anhydrous $LnCl_3$ with 3 equivalents of $Li[N(SiMe_3)_2]$ in tetrahydrofuran, with porphyrin free bases H_2porp and demonstrate that cationic lanthanide monoporphyrinate complexes can be synthesized *via* lanthanide amide complexes.

Results and discussion

Treatment of an excess of $Ln[N(SiMe_3)_2]_3 \cdot x[LiCl(THF)_3]$, generated *in situ* from the reaction of anhydrous $LnCl_3$ with 3 equivalents of $Li[N(SiMe_3)_2]$ in tetrahydrofuran, with porphyrin free bases in refluxing bis(2-methoxyethyl) ether–tetrahydrofuran solution (6 : 1 v/v) for 48 h yielded the cationic monoporphyrinate complexes $[Ln^{III}(TMPP)(H_2O)_3]Cl$ (Ln = Yb **1**, Er **2** or Y **3**) when the free base was H_2TMPP [5,10,15,20-tetrakis(*p*-methoxyphenyl)porphyrin] and $[Yb^{III}(TTP)(H_2O)_2(THF)]Cl$ **4** when the free base was H_2TTP [5,10,15,20-tetrakis(*p*-tolyl)porphyrin]. Compounds **1**–**4** were isolated as air-stable purple crystals in moderate yield. They all gave satisfactory elemental analyses and exhibited electronic absorption spectra characteristic of normal metal porphyrin complexes.[6] Their low-resolution mass spectra (FAB, positive-ion mode) exhibited peaks corresponding to the $[Ln(TMPP)]^+$ fragment. Their structures were established by X-ray crystallography. Attempts to synthesize the compounds *via* the interaction of $LnCl_3$ with the corresponding porphyrinate dianion, which gave a very complex reaction mixture, were met with failure.

Crystals of complexes **1**·4THF, **2**·4THF and **3**·4THF suitable for X-ray diffraction study were grown by slow evaporation of a solution of the respective compound in tetrahydrofuran. Perspective drawings of the compounds are shown in Figs. 1, 2 and 3, respectively. Compounds **1**, **2** and **3** are isomorphous and crystallized in the monoclinic space group *Cc* with a β angle close to 90°. Selected bond lengths and bond angles are shown in Table 1. Crystal structure analyses revealed that the lanthanide(III) ions are eight-co-ordinate, surrounded by four N atoms of the porphyrinate dianion and four aqua ligands in which two are disordered with site occupancy of 0.5 [O(3w) and O(4w) for **1** and **2**; O(2w) and O(4w) for **3**], and have a square antiprismatic co-ordination geometry. The average dihedral angles between a pair of N–Ln–N and O–Ln–O planes are 47.6, 41.7 and 42.3° for compounds **1**, **2** and **3**, respectively. The structural data are similar to those of the neutral terbium(III) monoporphyrinate complex $[Tb^{III}(\beta\text{-}Cl_8TPP)(O_2CMe)(Me_2SO)_2]$[5] in which the metal also adopts a square antiprismatic co-ordination geometry with the average dihedral angle between a pair of N–Tb–N and O–Tb–O planes being 46.7°. The average Ln–N and Ln–O bond lengths are 2.301 (Yb–N) and 2.307 Å (Yb–O) for **1**; 2.329 (Er–N) and 2.391 Å (Er–O) for **2** and 2.331 (Y–N) and 2.356 Å (Y–O) for **3**. The displacement of the lanthanide atoms from the mean planes formed by four N atoms and four O atoms are, respectively, 1.082 and 1.640 Å for **1**, 1.11 and 1.650 Å for **2**, 1.14 and 1.635 Å for **3**. The two mean planes are parallel to each other with a separation of 2.716, 2.757 and 2.777 Å for **1**, **2** and **3**, respectively. The increase in Ln–N and separation between the two

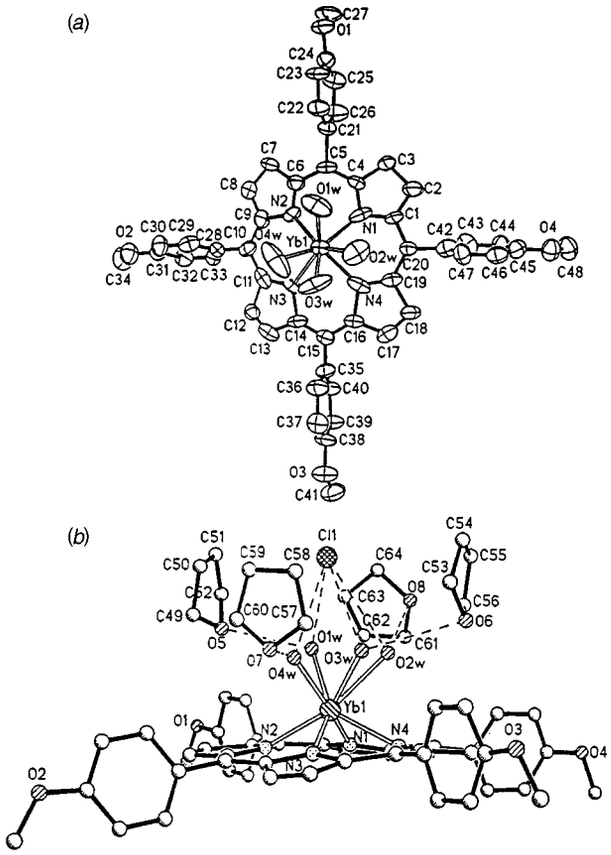

Fig. 1 (*a*) Perspective view of the cation of compound **1**. (*b*) A side view of the molecular structure of compound **1**.

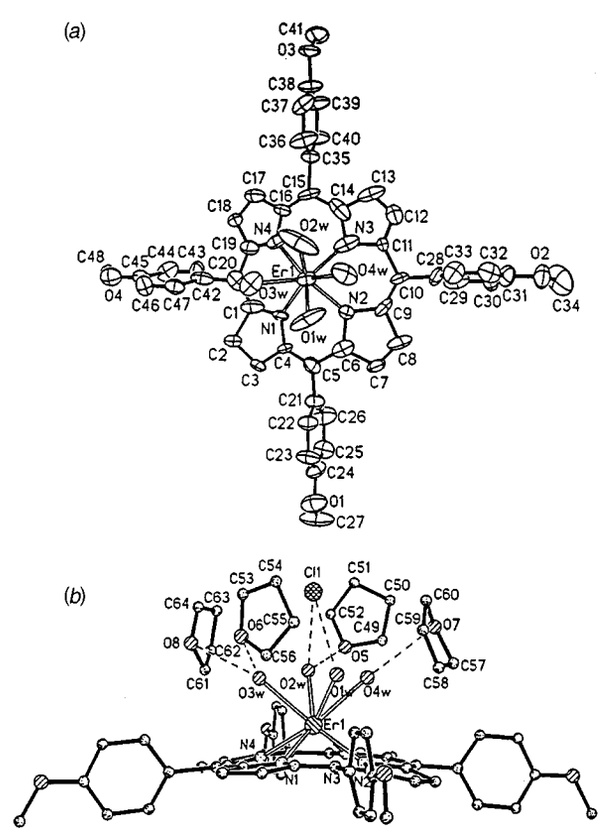

Fig. 2 (*a*) Perspective view of the cation of compound **2**. (*b*) A side view of the molecular structure of compound **2**.

parallel planes in the series $Yb^{III} < Er^{III} < Y^{III}$ reflect an increase in ionic radii: 98.5 < 100.4 < 101.9 pm (see Table 2).[7] Fig. 4 gives the projections along the Ct–Ln axes (Ct is the

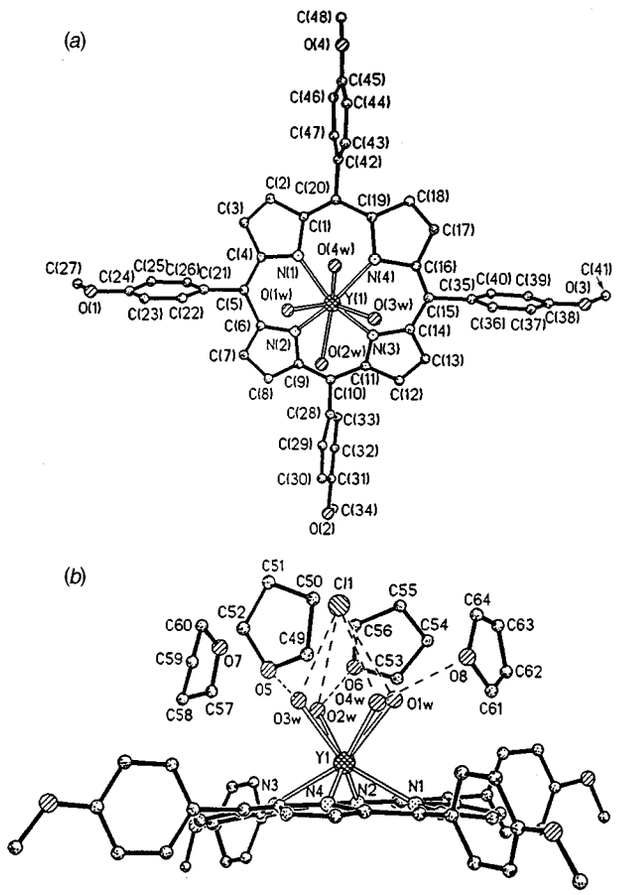

Fig. 3 (*a*) Perspective view of the cation of compound **3**. (*b*) A side view of the molecular structure of compound **3**.

centroid of the N_4 mean plane) of the cations of **1**, **2** and **3** without the aqua ligands. The porphyrin rings exhibit a saddle like distortion with the average perpendicular distance for the nitrogens, pyrrole α-carbons, pyrrole β-carbons and *meso*-carbons from the N_4 mean plane being *ca.* 0.03, 0.17, 0.28 and 0.12 Å for **1**, 0.04, 0.14, 0.29 and 0.15 Å for **2**, and 0.02, 0.12, 0.28 and 0.17 Å for **3**. The dihedral angles formed between the phenyl rings and the N_4 mean plane are 92.6 [C(21)–C(26)], 79.6 [C(28)–C(33)], 89.1 [C(35)–C(40)] and 102.1° [C(42)–C(47)] for **1**, 90.7 [C(35)–C(40)], 77.9 [C(42)–C(47)], 87.7 [C(21)–C(26)] and 101.0° [C(28)–C(33)] for **2**, and 87.4 [C(21)–C(26)], 80.6 [C(28)–C(33)], 84.5 [C(35)–C(40)] and 103.7° [C(42)–C(47)] for **3**. As shown by the edge-on view of the molecular structures [Figs. 1(*b*), 2(*b*) and 3(*b*)], the independent solvate THF molecules and the anionic Cl atom form acceptor hydrogen bonds with the aqua ligands. The average intermolecular distances between the aqua ligands and the chloride ion are 3.190, 3.068 and 3.226 Å for **1**, **2** and **3**, respectively, and the average intermolecular distances between the aqua ligands and solvate THF molecules are 2.971, 2.918 and 2.822 Å, respectively.

Crystals of complex **4**·3THF suitable for X-ray diffraction study were also grown by slow evaporation of a solution of **4** in tetrahydrofuran. A perspective view of **4**·3THF is shown in Fig. 5. The seven-co-ordinated Yb atom lies 1.090 Å above the mean plane defined by four N atoms and 1.676 Å below the plane defined by three O atoms [O(1) and O(2) of the two aqua ligands and O(3) of the THF molecule], while the two mean planes are parallel to each other with a separation of 2.762 Å. The co-ordination polyhedron about Yb is best described as a monocapped trigonal prism. Fig. 6(a) gives the projections along the Ct–Yb axis of the cation of **4** without the aqua ligands. As in **1**, the porphyrin ring of **4** also displays a saddle distortion with the average displacements of the nitrogens,

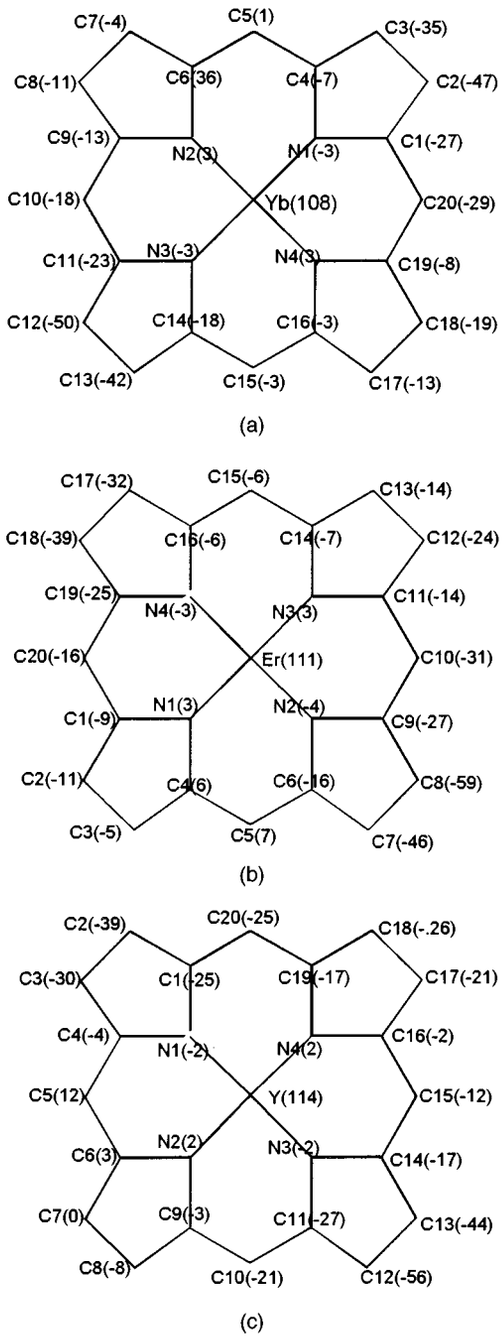

Fig. 4 Projections along the Ct–Ln axes (Ct is the centroid of the N_4 mean plane) of the cations of compounds **1**(a), **2**(b) and **3**(c) without the aqua ligands. The deviation of individual atoms from the N_4 mean plane is given in parentheses in units of 0.01 Å.

pyrrole α-, pyrrole *β*- and *meso*-carbons from the N_4 mean plane being *ca*. 0.004, 0.13, 0.31 and 0.15 Å, respectively. The dihedral angles formed between the phenyl rings and the N_4 mean plane are 87.4 [C(21)–C(26)], 79.6 [C(28)–C(33)], 89.1 [C(35)–C(40)] and 77.9° [C(42)–C(47)]. Intermolecular hydrogen bonds are also observed between the aqua ligands and the chloride ion [Cl · · · O(1) 3.061(8), Cl · · · O(2) 3.048(8) Å] and a solvate THF molecule [O(2) · · · O(4) 2.76(2) Å].

Metathesis of compound **1** with an excess of $AgBF_4$ in tetrahydrofuran led to the disproportionation of Ag^{I} to silver metal and Ag^{II}, and the isolation of the silver(II) porphyrin complex $[Ag^{II}(TMPP)]$ **5**. Compound **5** exhibited a parent peak at *m*/*z* 841 corresponding to the $[Ag(TMPP)]^+$ fragment for ^{109}Ag in its low-resolution mass spectrum (FAB positive-ion mode), and in chloroform solution exhibited a nine-line signal ($g = 2.062$, $A = 20.26$ G) in its room temperature EPR spectrum indicating

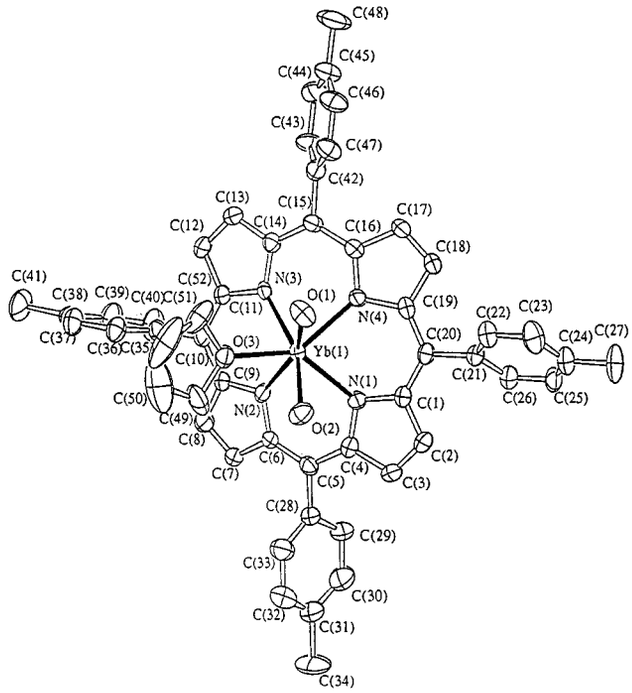

Fig. 5 Perspective view of the cation of compound **4**.

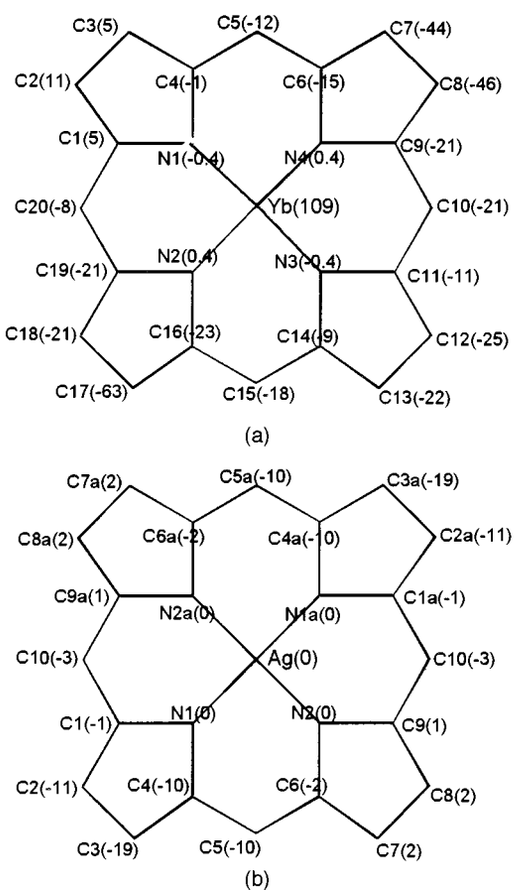

Fig. 6 (a) Projection along the Ct–Yb axis of the cation of compound **4** without the aqua ligands. (b) Projection along the Ct–Ag axis of compound **5**. The deviation of individual atoms from the N_4 mean plane is given in parentheses in units of 0.01 Å.

hyperfine splittings due to four equivalent ^{14}N nuclei. This indicates that the silver ion has a +2 oxidation state with a d^9 electronic configuration. The structure of **5** was established by X-ray crystallography. Suitable crystals of **5**·0.5CH_2Cl_2 were grown by slow evaporation of a solution of **5** in dichloro-

Table 1 Selected bond lengths (Å) and angles (°) for compounds **1**–**5**

	1	**2**	**3**	**4**	**5**
M–N(1)	2.266(9)	2.360(8)	2.273(11)	2.323(8)	2.098(5)
M–N(2)	2.311(5)	2.273(11)	2.369(11)	2.346(8)	2.090(5)
M–N(3)	2.362(5)	2.235(16)	2.415(10)	2.319(8)	
M–N(4)	2.271(10)	2.446(12)	2.267(11)	2.314(8)	
M–N[a]	2.303	2.329	2.331	2.326	2.094
M–O(1W)	2.343(8)	2.312(12)	2.332(10)	2.330(7)	—
M–O(2W)	2.441(7)	2.301(12)	2.36(2)	2.359(8)	—
M–O(3W)	2.262(9)	2.49(3)	2.293(13)	2.396(7)[b]	—
M–O(4W)	2.18(3)	2.46(2)	2.433(15)	—	—
M–O[a]	2.307	2.391	2.355	2.362	—
For skeleton atoms (average values)[c]					
$N–C_\alpha$	1.389	1.380	1.407	1.385	1.361
$C_\alpha–C_\beta$	1.296	1.415	1.448	1.435	1.440
$C_\beta–C_\beta$	1.400	1.346	1.357	1.343	1.338
$C_\alpha–C_m$	1.400	1.402	1.397	1.405	1.403
$C_\alpha–N–C_\alpha$	105.8	104.3	107.8	106.2	109.2
$N–C_\alpha–C_\beta$	109.4	109.8	108.5	109.1	107.8
$C_\alpha–C_\beta–C_\beta$	107.6	108	107.5	107.7	107.8
$C_\alpha–C_m–C_\alpha$	125.4	127.9	124.1	125.6	126.8
$N–C_\alpha–C_m$	125.0	123.1	126.6	125.3	126.1
$C_\beta–C_\alpha–C_m$	125.3	126.8	124.6	125.2	126.3

[a] M–N and M–O are average bond distances of the metal to the N atoms of the porphyrin ring and O atoms of water molecules, respectively. [b] Bond length between Yb and the O atom of the co-ordinated tetrahydrofuran molecule. [c] C_α, C_β and C_m denote the α- and β-carbon atoms of the pyrrole ring and the *meso*-carbon atom, respectively.

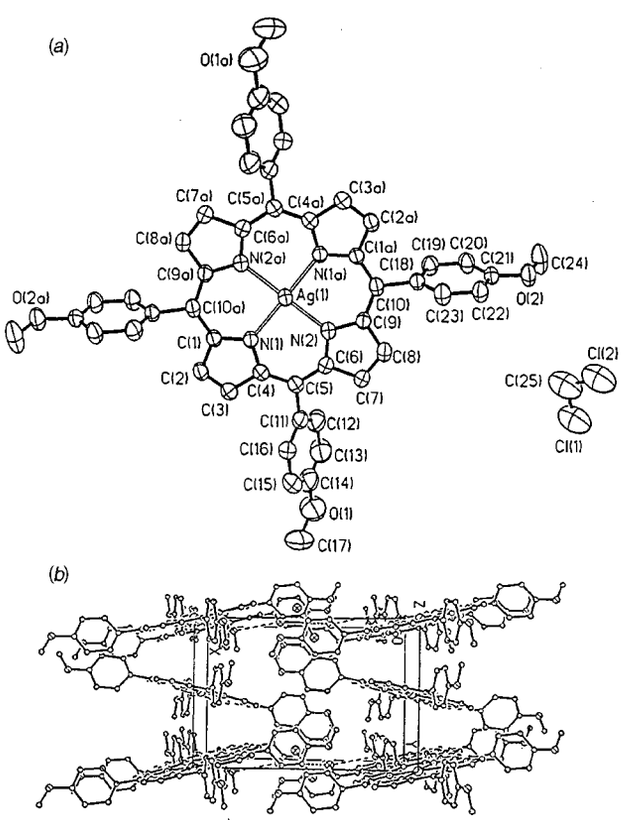

Fig. 7 (*a*) Perspective view of the molecular structure of compound **5**. (*b*) The packing diagram of compound **5**.

methane. A perspective drawing of **5** is shown in Fig. 7(*a*). The solid state structure reveals that it is monomeric. The square planar silver(II) complex has C_i symmetry with the Ag atom in the porphyrin plane and coplanar with four N atoms. Fig. 6(*b*) gives the projection of compound **5** along the Ct–Ag axis. The average perpendicular distances for the pyrrole α-, pyrrole β- and *meso*-carbons from the N_4 mean plane are *ca*. 0.04, 0.08, and 0.07 Å, respectively. The dihedral angles

Table 2 Additional geometrical parameters for metal monoporphyrinate complexes

	1	**2**	**3**	**4**	**5**
Orientation of the macrocycles[a]/°					
	47.6	41.7	42.3		—
Distances of mean planes[b]/Å					
$M–(N_p)_4$	1.08	1.11	1.14	1.09	0.00
$M–(O_p)_4$	1.640	1.650	1.635		—
Inclination of the pyrrole rings[c]/°					
	11.1	4.6	10.0	2.7	4.9
	4.7	12.7	2.7	11.9	0.8
	11.6	5.8	13.0	6.3	—
	5.0	10.0	7.0	16.6	—
Ionic radius of the metal ions[d]/pm					
	98.5	100.4	101.9	98.5	

[a] The average dihedral angles of adjacent N–M–N and O–M–O planes that indicate the staggered configuration of water molecules with the porphyrin ring. [b] $(N_p)_4$ and $(O_p)_4$ denote the mean planes of the four N atoms of a porphyrin ring and four water molecules, respectively. [c] The dihedral angles of the mean planes of the pyrrole rings with the $(N_p)_4$ planes. [d] For lanthanide ions with co-ordination number 8 taken from Shannon.[7]

formed between the phenyl rings and the N_4 mean plane are 120.0 [C(11)–C(16)] and 101.8° [C(18)–C(23)]. The cavity of the porphyrin pocket has a diameter of *ca*. 4.2 Å. The Ag–N distances are 2.090(5) and 2.098(5) Å and are comparable to those of [Ag^{II}(TPP)] [2.082(3) and 2.101(3) Å].[8] The asymmetric unit contains one-half of a [Ag^{II}(TMPP)] molecule and a disordered CH_2Cl_2 molecule with site occupancy 1/4. The [Ag^{II}(TMPP)] molecules are arranged in layers with the dihedral angle between adjacent layers being 31.4° as shown in Fig. 7(*b*). The relatively high *R* value is due to the poor quality of the crystal.

Catalysis

Compound **1**, at 30 °C for 24 h, catalysed the conversion of

Table 3 The living property of the catalyst

Cycle	Conversion (%)
1st	100
2nd	100
3rd	100
4th	91.7
5th	75.0

Catalyst: $[Yb^{III}(TMPP)(H_2O)_3]Cl$, 0.023 g ($1.77 \times 10^{-2}$ mmol). Monomer: phenyl isocyanate, 0.636 g (5.34 mmol). Cyclic trimer: 1,3,5-triphenyl-*s*-triazine-2,4,6-trione. Reaction conditions: each cycle was allowed to proceed for 24 h at 30 °C. In the initial cycle the catalyst and the monomer were mixed at a molar ratio of 1 : 300. In successive cycles the same amount of monomer was added to the residue of the previous cycle after removal of volatile materials. The yield was calculated based on the weight difference before and after the reaction.

phenyl isocyanate into its cyclic trimer, 1,3,5-triphenyl-*s*-triazine-2,4,6-trione, quantitatively even at a catalyst to monomer mole ratio as low as 1 : 600. It behaves, to a certain extent, as a living catalyst for the cyclotrimerization process. When **1** was mixed with phenyl isocyanate at 1 : 300 ratio, after 24 h at 30 °C, the resultant mixture could still act as a catalyst for the cyclotrimerization. Results of the living catalyst studies given in Table 3 show that compound **1** can catalyse the transformation quantitatively for the first three cycles without losing any of its activity. Its activity eventually decreased with the conversion being 91.7 and 75% in the fourth and fifth cycle, respectively. A possible mechanism for the catalytic process is shown in Scheme 1. Compound **1** reacted with phenyl isocyanate to

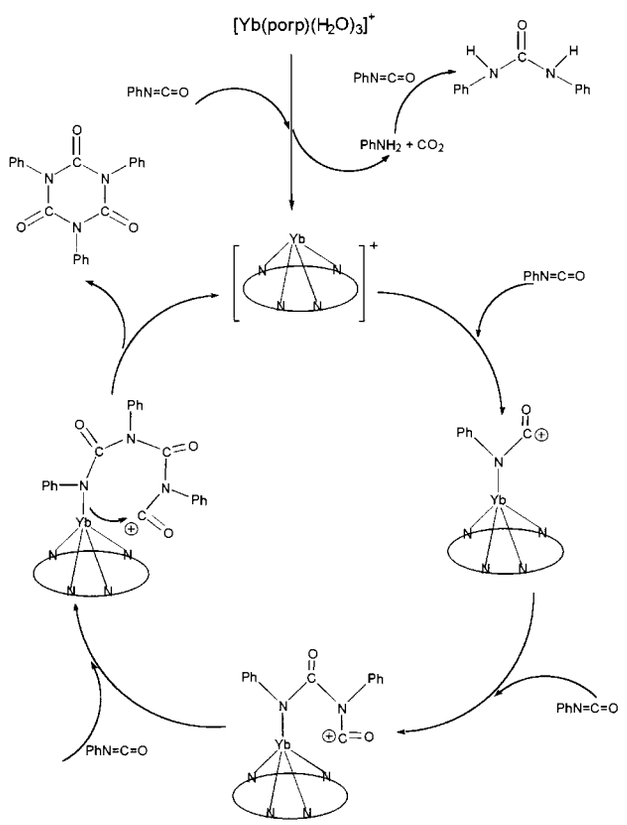

Scheme 1 Proposed mechanism for the cyclotrimerization of phenyl isocyanate.

generate aniline and the co-ordinatively unsaturated cationic species $[Yb(TMPP)]^+$. Aniline reacted with phenyl isocyanate to give carbanilide (1,3-diphenylurea). The ion $[Yb(TMPP)]^+$ then acted as a Lewis acid, catalysing the transformation of phenyl isocyanate to its cyclic trimer. The isolation of carbanilide from the reaction mixture supports the formation of aniline from the reaction of **1** with phenyl isocyanate. It is well known that isocyanates form the corresponding cyclic trimers in the presence of basic catalysts such as amines, alkoxides, organometallic compounds, *etc*.;[9] however, the use of a Lewis acid to catalyse the cyclotrimerization process has not been reported. As a control to test whether aniline was responsible for the catalytic cyclotrimerization process, aniline was allowed to react with phenyl isocyanate at a mole ratio of 1 : 150 at 30 °C. Carbanilide was produced as soon as aniline was mixed with phenyl isocyanate. However, no further reaction was observed even after 48 h. This demonstrates that aniline is not the active catalyst for the transformation, and suggests that the co-ordinatively unsaturated cationic ytterbium porphyrinate complex, generated *in situ*, is responsible for the cyclotrimerization process. Recently, neutral organolanthanide amide complexes have been reported to catalyse the polymerization of phenyl isocyanate.[10] Here we have demonstrated that the cationic ytterbium porphyrinate complex, presumably acting as a Lewis acid, catalyses the cyclotrimerization of phenyl isocyanate. However, compounds **2** and **3** did not catalyse the cyclotrimerization.

In this paper we have shown that cationic lanthanide(III) monoporphyrinate complexes can be prepared *via* the protonolysis of lanthanide amide complexes with porphyrin. Notably compounds **1**–**4** are the first structurally characterized lanthanide(III) monoporphyrinate complexes comprising a discrete lanthanide(III) monoporphyrinate cation and a discrete chloride anion. We have further demonstrated that compound **1** is capable of catalysing the cyclotrimerization of phenyl isocyanate and propose a cationic cyclotrimerization mechanism for the transformation.

Experimental

Procedures

All reactions were carried out in an atmosphere of dry nitrogen. Solvents were dried by standard procedures, distilled and deaerated prior to use. All chemicals used were of reagent grade, obtained from the Aldrich Chemical Company, and, where appropriate, degassed before use. 5,10,15,20-Tetrakis(*p*-methoxyphenyl)porphyrin (H_2TMPP) and 5,10,15,20-tetrakis(*p*-tolyl)porphyrin (H_2TTP) were prepared according to literature methods.[11] The compound $Ln[N(SiMe_3)_2]_3 \cdot x[LiCl(THF)_3]$ was generated *in situ* according to the literature procedure.[12] Microanalyses were performed by the Shanghai Institute of Organic Chemistry, Chinese Academy of Sciences. The IR spectra (KBr pellets) were recorded on a Hitachi 270-30 or on a Nicolet Nagna-IR 550 spectrometer, electronic absorption spectra in the UV/VIS region on a OLIS Cary 15 spectrophotometer and NMR spectra on a JEOL EX270 spectrometer. Chemical shifts of ^1H and ^{13}C-{^1H} NMR spectra were referenced to internal deuteriated solvents and then recalculated to TMS (δ 0.00). The EPR spectra were obtained with an X-band JEOL JES TE-100 spectrometer at room temperature, low resolution mass spectra (LRMS) on a Finnigan MAT SSQ-710 or MAT 95 spectrometer in FAB (positive) mode and GC-MS spectra on a HP5890A GC-MSD spectrometer.

Preparations

Compounds **1**–**4** were prepared by the same procedure. A typical procedure is given for **1**.

$[Yb^{III}(TMPP)(H_2O)_3]Cl$ 1. A solution of *n*-BuLi (1.6 M, 9.5 cm^3, 15.2 mmol) in hexane was added dropwise over a period of 10 min to a solution of $(Me_3Si)_2NH$ (2.45 g, 15.2 mmol) in tetrahydrofuran (20 cm^3), the reaction mixture was allowed to stir at room temperature for 2 h, then transferred slowly to a suspension of $YbCl_3$ (1.40 g, 5.0 mmol) in tetrahydrofuran (20

cm^3). After stirring at room temperature for 24 h the mixture was centrifuged and filtered. The solvent of the filtrate was concentrated *in vacuo* to *ca*. 5 cm^3, then added to a solution of H_2TMPP (0.73 g, 1.0 mmol) in bis(2-methoxyethyl) ether (30 cm^3). The resultant solution was refluxed. The progress of the reaction was monitored by UV–VIS spectroscopy. After refluxing for 48 h the solution was cooled to room temperature and filtered, and the residue extracted with dichloromethane (3 × 10 cm^3). The solvent of the combined filtrate was removed *in vacuo* to give a purple residue. This was washed with *n*-hexane (2 × 10 cm^3) and diethyl ether (2 × 10 cm^3), extracted with tetrahydrofuran (3 × 10 cm^3) and filtered. The filtrate was concentrated *in vacuo* to *ca*. 15 cm^3 and then allowed to evaporate slowly in air to give purple crystals which were filtered off and dried *in vacuo*. Yield: 0.91 g, 85%. mp > 300 °C (Found: C, 58.3; H, 4.5; Cl, 3.2; N, 5.2. Calc. for $C_{48}H_{42}ClN_4O_7Yb\cdot C_4H_8O$: C, 58.5; H, 4.7; Cl, 3.3; N, 5.2%.). IR (cm^{-1}, in KBr): 3347 (br) w, 3014w, 2952w, 2853w, 1606s, 1572m, 1519s, 1507s, 1480m, 1463m, 1439m, 1412w, 1330m, 1288m, 1247vs, 1174s, 1111w, 1074w, 1033m, 992s, 856w, 804s, 790m, 755m, 729m, 671w, 640w, 600m and 538w. UV–VIS in $CHCl_3$, 20 °C, [λ_{max}/nm, log(ε/dm^3 mol^{-1} cm^{-1}) in parentheses]: 425 (5.60), 553 (4.32) and 593 (3.94). Positive-ion FAB mass spectrum: *m*/*z* 906, $[Yb(TMPP)]^+$ for ^{174}Yb.

$[Er^{III}(TMPP)(H_2O)_3]Cl$ 2. *n*-Butyllithium (1.6 M, 3.7 cm^3, 5.92 mmol), $(Me_3Si)_2NH$ (0.95 g, 5.92 mmol), $ErCl_3$ (0.54 g, 1.97 mmol) and H_2TMPP (0.23 g, 0.31 mmol) were used. Yield: 0.24 g, 69%, purple-red crystals; mp > 300 °C. (Found: C, 53.3; H, 3.9; N, 5.0. Calc. for $C_{48}H_{42}ClErN_4O_7\cdot 1.5CH_2Cl_2$: C, 53.2; H, 4.0; N, 5.0%). IR (cm^{-1}, in KBr): 3423 (br) s, 3014w, 2952w, 2853w, 1630m, 1605s, 1518m, 1480w, 1461w, 1439m, 1406w, 1329m, 1290m, 1247vs, 1174s, 1105w, 1074w, 1033m, 990s, 847w, 802vs, 729w, 600m and 538w. UV–VIS in $CHCl_3$, 20 °C, [λ_{max}/nm, log(ε/dm^3 mol^{-1} cm^{-1}) in parentheses]: 425 (5.42), 552 (4.23) and 593 (4.00). Positive-ion FAB mass spectrum: *m*/*z* 917, $[Er(TMPP)(H_2O) + 1]^+$; 899, $[Er(TMPP) + 1]^+$; 735, $[H_2(TMPP) + 1]$ for ^{166}Er.

$[Y^{III}(TMPP)(H_2O)_3]Cl$ 3. *n*-Butyllithium (1.6 M, 3.7 cm^3, 5.92 mmol), $(Me_3Si)_2NH$ (0.95 g, 5.92 mmol), YCl_3 (0.39 g, 2.00 mmol) and H_2TMPP (0.25 g, 0.34 mmol) were used. Yield: 0.28 g, 72%, purple-red crystals, mp > 300 °C (Found: C, 60.2; H, 5.3; N, 5.0. Calc. for $C_{48}H_{42}ClN_4O_7Y\cdot 2C_4H_8O\cdot CH_2Cl_2$: C, 60.0; H, 5.3; N, 4.9%). IR (cm^{-1}, in KBr): 3419 (br) vs, 3014w, 2952w, 2853w, 1631s, 1605s, 1518s, 1505s, 1477m, 1463m, 1439m, 1408w, 1328m, 1286m, 1247vs, 1174s, 1107w, 1064w, 1029m, 990s, 849w, 807s, 790m, 755m, 729m, 671w, 640w, 600m, 540w and 424w. ^1H NMR (d_6-acetone): phenyl protons, δ 8.79 (8 H, br s) and 7.35 (8 H, br s); pyrrole protons, δ 8.25 (4 H, br s) and 7.98 (4 H, br s); methoxy protons, δ 4.07 (12 H, br m); water protons, δ 2.86 (6 H, br s). UV-VIS in $CHCl_3$, 20 °C [λ_{max}/nm, log(ε/dm^3 mol^{-1} cm^{-1}) in parentheses]: 424 (5.29), 454 (4.36) and 555 (4.14). Positive-ion FAB mass spectrum: *m*/*z* 897, 856, $[Y(TMPP)(H_2O)(OH)]^+$; 838, $[Y(TMPP)(OH)]^+$; 821, $[Y(TMPP)]^+$ for ^{89}Y.

$[Yb^{III}(TTP)(H_2O)_2(THF)]Cl$ 4. *n*-Butyllithium (1.6 M, 5.0 cm^3, 8.0 mmol), $(Me_3Si)_2NH$ (1.29 g, 8.0 mmol), $YbCl_3$ (0.75 g, 2.68 mmol) and H_2TTP (0.36 g, 0.53 mmol) were used. Yield: 0.39 g, 71%, purple-red crystals, mp > 300 °C (Found: C, 60.2; H, 5.0; Cl, 3.0; N, 5.3. Calc. for $C_{52}H_{48}ClN_4O_3Yb\cdot 3H_2O$: C, 60.1; H, 5.2; Cl, 3.4 N, 5.4%). IR (cm^{-1}, in KBr): 3356 (br) w, 3026w, 2915w, 2878w, 1615 (br) m, 1520m, 1508w, 1479m, 1449w, 1401w, 1329m, 1202m, 1182m, 1107m, 1067m, 1005m, 992s, 845w, 804s, 798s, 723m, 578w, 523m and 417w. UV–VIS in $CHCl_3$, 20 °C, [λ_{max}/nm, log(ε/dm^3 mol^{-1} cm^{-1}) in parentheses]: 422 (5.76), 551 (4.51) and 589 (3.97). Positive-ion FAB mass spectrum: *m*/*z* 859, $[Yb(TTP)(OH)]^+$; 842, $[Yb(TTP)]^+$ for ^{174}Yb.

$[Ag^{II}(TMPP)]$ 5. An excess of $AgBF_4$ (0.1 g, 0.514 mmol) was added to a solution of complex **1** (0.21 g, 0.187 mmol) in tetrahydrofuran (40 cm^3). The solution was allowed to react for 24 h at room temperature to give a black metallic powder, then filtered. The solvent of the filtrate was removed *in vacuo* to give a dark purple residue. The residue was redissolved in the minimum volume of $CHCl_3$ and chromatographed on a silica gel column (2 × 10 cm). A dark red band and a dark purple band were obtained when the column was eluted with $CHCl_3$ and acetone solution, respectively. Removal of solvent from the dark red band gave a dark red residue. This was redissolved in the minimum volume of $CHCl_3$ and filtered. The filtrate was allowed to evaporate slowly to give dark red crystals which were filtered off and dried *in vacuo*. Yield: 0.04 g, 25%, dark red crystals; mp > 300 °C (Found: C, 62.2; H, 3.8; N, 5.3. Calc. for $C_{48}H_{36}AgN_4O_4\cdot\frac{3}{4}CHCl_3$: C, 62.2; H, 3.9; N, 6.0%). IR (cm^{-1}, in KBr): 3398 (br) m, 3026w, 2958w, 2931w, 2835w, 1772w, 1717m, 1604s, 1574w, 1509s, 1471m, 1440w, 1339w, 1250vs, 1173s, 1105w, 1069w, 1033m, 1005s, 966w, 883w, 845m, 803s, 765w, 714w, 671w, 602w and 538w. UV–VIS in $CHCl_3$, 20 °C, [λ_{max}/nm, log(ε/dm^3 mol^{-1} cm^{-1}) in parentheses]: 241 (4.47), 321 (4.28), 429 (5.07) and 544 (3.82). EPR (chloroform) : $g = 2.062$, nine-line pattern with hyperfine splitting of *ca*. 20.26 G. Positive-ion FAB mass spectrum: *m*/*z* 841, $[Ag(TMPP)]^+$; 735, $[(H_2TMPP) + 1]^+$ for ^{109}Ag.

Attempts to isolate an identifiable product from the dark purple acetone band were unsuccessful.

Catalysis

Compound **1** (0.023 g, 1.77×10^{-2} mmol) and freshly distilled phenyl isocyanate (0.0636 g, 5.34 mmol) were transferred to an oven dried preweighed 5 cm^3 vial under nitrogen to give a purple-red solution. The vial was then weighed. The solution solidified after standing at 30 °C for 24 h. Volatile material was then removed *in vacuo* at 100 °C until a constant weight was obtained. The vial together with its solid residue was then weighed. The yield was calculated based on the weight difference before and after the reaction. Methanol was added to the resultant solid to quench the reaction to give a purple-red solution and white solids. The solution was filtered and the white solids were extracted with methanol (2 × 5 cm^3). The combined methanol solution was concentrated to *ca*. 5 cm^3 and cooled to −20 °C to give white crystals of carbanilide whose authenticity was confirmed by comparing its melting point, IR, ^1H and 13C NMR and mass spectra with the literature. The methanol insoluble white solid was then dissolved in chloroform and analysed by GC-MS as pure 1,3,5-triphenyl-*s*-triazine-2,4,6-trione. The authenticity of the compound which recrystallized as colourless crystals in chloroform was confirmed by comparing its melting point, IR, ^1H and ^{13}C NMR and mass spectra with the literature.[13]

For the living catalyst study, the reaction was carried out as above with compound **1** (0.023 g, 1.77×10^{-2} mmol) and phenyl isocyanate (0.636 g, 0.58 cm^3, 5.34 mmol) at a mole ratio of 1 : 300. However, after removal of the volatile materials, rather than quenching the reaction with methanol, 300 equivalents of phenyl isocyanate (0.636 g, 0.58 cm^3, 5.34 mmol) were added to the residue. The resultant mixture was allowed to react for 24 h at 30 °C. The same procedure was repeated for a total of 5 cycles. At the end of each cycle the yield was calculated based on the weight difference before and after the reaction.

X-Ray crystallography

Pertinent crystallographic data and other experimental details are summarized in Table 4. Crystals of compounds **1**–**4** suitable for X-ray diffraction study were grown by slow evaporation of a solution of the respective compound in tetrahydrofuran. Suit-

Table 4 Crystallographic data for compounds **1**–**5**

	1	**2**	**3**	**4**	**5**
Empirical formula	$C_{64}H_{74}ClN_4O_{11}Yb$	$C_{64}H_{74}ClErN_4O_{11}$	$C_{64}H_{74}ClN_4O_{11}Y$	$C_{64}H_{72}ClN_4O_6Yb$	$C_{8.5}H_{37}AgClN_4O_4$
Formula weight	1283.8	1278.0	1199.6	1201.8	883.1
Color and habit	Red prism	Dark red plate	Dark red prism	Purple block	Red plate
Crystal size/mm	0.22 × 0.32 × 0.40	0.08 × 0.35 × 0.42	0.10 × 0.25 × 0.40	0.19 × 0.29 × 0.40	0.05 × 0.30 × 0.40
Crystal system	Monoclinic	Monoclinic	Monoclinic	Triclinic	Monoclinic
Space group	*Cc* (no. 9)	*Cc* (no. 9)	*Cc* (no. 9)	*P*1 (no. 2)	$P2_1/c$ (no. 14)
a/Å	18.063(1)	18.101(3)	18.089(1)	14.484(1)	14.557(3)
b/Å	19.174(1)	19.202(3)	19.174(1)	14.489(1)	9.555(2)
c/Å	17.562(1)	17.597(3)	17.578(1)	14.893(1)	15.662(3)
α/°	—	—	—	76.15(1)	—
β/°	90.18(1)	90.32(1)	90.13(1)	88.59(1)	99.44(3)
γ/°	—	—	—	79.06(1)	—
V/Å^3	6082.4(6)	6116.2(6)	6096.7(6)	2978.7(4)	2149.0(8)
Z	4	4	4	2	2
F(000)	2644	2636	2520	1238	904
D_c/g cm^{-3}	1.402	1.388	1.185	1.340	1.365
μ/mm^{-1}	1.644	1.478	1.050	1.246	0.580
Transmission factors	0.924 to 1.079	0.865 to 1.173	0.894 to 1.000	0.855 to 1.149	0.919 to 1.118
2θ range/°	4–52	4–52	3–52	3–51	4–52
Reflections collected	9417	8858	6164	29875	5733
Independent reflections, *n* (R_{int})	5388 (0.0321)	4978 (0.0472)	6164 (0.00)	9955 (0.042)	3325 (0.0329)
Observed reflections, $I>m\sigma(I)$	5067, *m*=2	4507, *m*=2	1799, *m*=2	6587, *m*=3	2891, *m*=2
No. parameters, *p*	740	740	740	570	271
*R*1	0.0384	0.0525	0.0608	0.054	0.0723
*wR*2	0.0984	0.1384	0.1253	0.075	0.2063
S (goodness of fit)	1.004	1.026	0.870	1.33	1.179
$\Delta\rho_{max}$/e Å^{-3}	0.412, −0.600	0.605, −0.761	0.254, −0.558	1.06, −0.35	0.803, −0.644

able crystals of **5** were grown by slow evaporation of a solution of it in dichloromethane. The crystals were all wrapped in epoxy glue to prevent them from losing solvent, and attached on a thin glass stem. They were stable during the data collection. Intensity data of **1**, **2** and **5** were collected at 294 K on a MSC/Rigaku RAXIS IIC imaging plate diffractometer using Mo-Kα radiation ($\lambda = 0.71073$ Å) from a Rigaku RU-200 rotating-anode generator operating at 50 kV and 90 mA.[14] A self-consistent semiempirical absorption correction based on Fourier coefficient fitting of symmetry-equivalent reflections was applied by using the ABSCOR program.[15] Intensity data of **3** were collected in the variable ω-scan mode on a Rigaku AFC7R four-circle diffractometer using Mo-Kα radiation ($\lambda = 0.71073$ Å) at 294 K. The crystal class and orientation matrix were determined according to established procedures.[16] Unit-cell parameters were calculated from least-squares fitting of 2θ angles for 25 selected reflections. Crystal stability was monitored by recording three check reflections at intervals of 150 data measurements, and no significant variation was detected. The raw data were processed with a learn-profile procedure,[17] and empirical absorption corrections were applied by fitting a pseudo-ellipsoid to the ψ-scan data of selected strong reflections over a range of 2θ angles.[18] Intensity data of **4** were collected on a MAR research image plate scanner using graphite-monochromated Mo-Kα radiation ($\lambda = 0.71073$ Å) at 294 K; sixty 3° frames with an exposure time of 5 min per frame were used.

The structures of complexes **1**, **2**, **3** and **5** were solved by direct methods using the program package SHELXTL PLUS[19] and refined against F^2 by full matrix least-squares analysis using SHELXL 93.[20] The structure of **4** was solved by Patterson methods (DIRDIF 92 PATTY) and refined by full matrix least-squares analysis using the TEXSAN package.[21] All non-hydrogen atoms including disordered atoms were refined anisotropically by full-matrix least squares. Hydrogen atoms were generated in their idealized positions (C–H bond fixed at 0.96 Å for compounds **1**, **2**, **3** and **5**, at 0.95 Å for **4**), assigned appropriate isotropic thermal parameters, and allowed to ride on their respective parent carbon atoms. All hydrogen atoms were held stationary and included in structure factor calculations in the final stage of full-matrix least squares refinement.

CCDC reference number 186/1282.

Acknowledgements

Thanks are due to the Hong Kong Baptist University and the Hong Kong Research Grants Council (HKBU 142/95P and CUHK 303/96P) for financial support.

References

1 (*a*) C.-P. Wong, R. F. Venteicher and W. D. Horrocks, Jr., *J. Am. Chem. Soc.*, 1974, **96**, 7149; (*b*) W. D. Horrocks, Jr., R. F. Venteicher, C. A. Spilburg and B. L. Vallee, *Biochem. Biophys. Res. Commun.*, 1975, **64**, 317; (*c*) C.-P. Wong and W. D. Horrocks, Jr., *Tetrahedron Lett.*, 1975, 2637; (*d*) W. D. Horrocks, Jr. and C.-P. Wong, *J. Am. Chem. Soc.*, 1976, **98**, 7157; (*e*) L. A. Martarano, C.-P. Wong, W. D. Horrocks, Jr. and A. M. P. Goncalves, *J. Phys. Chem.*, 1976, **80**, 2389; (*f*) W. D. Horrocks, Jr. and E. G. Hove, *J. Am. Chem. Soc.*, 1978, **100**, 4386.

2 J. W. Buchler, A. De Cian, J. Fischer, M. Kihn-Botulinski, H. Paulus and R. Weiss, *J. Am. Chem. Soc.*, 1986, **108**, 3652; J. W. Buchler, A. De Cian, J. Fischer, M. Kihn-Botulinski and R. Weiss, *Inorg. Chem.*, 1988, **27**, 339; G. A. Spyroulias, A. G. Coutsolelos, C. P. Raptopoulou and A. Terzis, *Inorg. Chem.*, 1995, **34**, 2476 and refs. therein.

3 M. Moussavi, A. De Cian, J. Fischer and R. Weiss, *Inorg. Chem.*, 1986, **25**, 2107; D. Chabach, M. Lachkar, A. De Cian, J. Fischer and R. Weiss, *New J. Chem.*, 1992, **16**, 431; D. Chabach, M. Tahiri, A. De Cian, J. Fischer, R. Weiss and M. El Malouli Bibout, *J. Am. Chem. Soc.*, 1995, **117**, 8548 and refs. therein.

4 C. J. Schaverien and A. G. Orpen, *Inorg. Chem.*, 1991, **30**, 4968.

5 G. A. Spyroulias, A. Despotopoulos, C. P. Raptopoulou, A. Terzis and A. G. Coutsolelos, *Chem. Commun.*, 1997, 783.

6 K. Kalyanasundaram, *Photochemistry of Polypyridine and Porphyrin Complexes*, Academic Press, London, 1992, p. 376.

7 R. D. Shannon, *Acta Crystallogr., Sect. A*, 1976, **32**, 751.

8 W. R. Scheidt, J. U. Mondal, C. W. Eigenbrot, A. Adler, L. J. Radonovich and J. L. Hoard, *Inorg. Chem.*, 1986, **25**, 795.

9 J. Mizuya, T. Yokozawa and T. Endo, *J. Polym. Sci., Part A : Polym. Chem.*, 1991, **29**, 1545 and refs. therein.

10 L. Mao, Q. Shen, M. Xue and J. Sun, *Organometallics*, 1997, **16**, 3711.

11 A. D. Adler, F. R. Longo, J. D. Finarelli, J. Goldmacher, J. Assour and L. Korsakoff, *J. Org. Chem.*, 1967, **32**, 476; J. S. Lindsey, I. C. Schreiman, H. C. Hsu, P. C. Kearney and A. M. Marguerettaz, *J. Org. Chem.*, 1987, **52**, 827.
12 D. C. Bradley, J. S. Ghotra and F. A. Hart, *J. Chem. Soc.*, *Dalton Trans.*, 1973, 1021; V. Lorenz, A. Fischer, K. Jacob, W. Brüser, T. Gelbrich, P. G. Jones and F. T. Edelmann, *Chem. Commun.*, 1998, 2217.
13 Y. Nambu and T. Endo, *J. Org. Chem.*, 1993, **58**, 1932; I. E. Jones and N. G. Savill, *J. Chem. Soc.*, 1957, 4392.
14 J. Tanner and K. Krause, *The Rigaku Journal*, 1994, **11**, 4; 1990, **7**, 28; K. L. Krause and G. N. Phillips, Jr., *J. Appl. Crystallogr.*, 1992, **25**, 146; M. Sato, M. Yamamoto, K. Imada, Y. Katsube, N. Tanaka and T. Higashi, *J. Appl. Crystallogr.*, 1992, **25**, 348.
15 T. Higashi, ABSCOR, An Empirical Absorption Correction Based on Fourier Coefficient Fitting, Rigaku Corporation, Tokyo, 1995.
16 R. A. Sparks, in *Crystallographic Computing Techniques*, ed. F. R. Ahmed, Munksgaard, Copenhagen, 1976, p. 452.
17 R. Diamond, *Acta Crystallogr.*, *Sect. A*, 1968, **25**, 43.
18 G. Kopfmann and R. Huber, *Acta Crystallogr.*, *Sect. A*, 1968, **24**, 348.
19 G. M. Sheldrick, *SHELXL PC Manual*, Siemens Analytical X-Ray Instruments, Inc., Madison, WI, 1990; *Computational Crystallography*, ed. D. Sayre, Oxford University Press, New York, 1982, p. 506; *Crystallographic Computing 3: Data Collection, Structure Determination, Proteins, and Databases*, eds. G. M. Sheldrick, C. Kruger and R. Goddard, Oxford University Press, New York, 1985, p. 175.
20 G. M. Sheldrick, SHELXL 93, Program for Crystal Structure Refinement, University of Göttingen, 1993; *Crystallographic Computing 6: A Window on Modern Crystallography*, eds. H. D. Flack, L. Parkanyi and K. Simon, Oxford University Press, New York, 1993.
21 TEXSAN, Crystal Structure Analysis Package, Molecular Structure Corporation, Houston, TX, 1985, 1992.

Paper 8/09696A